ACS Catalysis

Research Article

pubs.acs.org/acscatalysis

Fischer–Tropsch Synthesis: Effects of Hydrohalic Acids in Syngas on a Precipitated Iron Catalyst

Wenping Ma,[†] Gary Jacobs,[†] Gerald A. Thomas,[†] Wilson D. Shafer,[†] Dennis E. Sparks,[†] Hussein H. Hamdeh,[‡] and Burtron H. Davis*[,†]

[†]Center for Applied Energy Research, University of Kentucky, 2540 Research Park Drive, Lexington, Kentucky 40511, United States
[‡]Department of Physics, Wichita State University, 1845 Fairmount, Wichita, Kansas 67260, United States

ABSTRACT: The current investigation was undertaken to identify limits of hydrohalic acid (HX, X = F, Cl, Br) impurities in syngas and shed light on the mechanism of HX poisoning of a 100 Fe/5.1 Si/2 Cu/3 K FTS catalyst under industrially relevant conditions using a 1-L slurry-phase reactor. Co-feeding <2.0 ppm of HCl or HBr in syngas for 72–170 h did not significantly deactivate the Fe catalyst. On the other hand, cofeeding 3.0–5.0 ppm of HCl or HBr in syngas for a similar time period resulted in slow deactivation. A higher tolerance, that is, 5–10 ppm, was observed for HF, indicating a weaker poisoning effect. In all cases, rapid deactivation was accompanied by decreases in C_{5+} and CO_2 selectivities at higher levels of HX (i.e., 20 ppm and above). Mössbauer spectroscopy and XRD were used to study the Fe phases in the catalyst before and after deactivation induced by each of the HX poisons. Results of Mössbauer spectroscopy suggest that an adsorptive mechanism is responsible for the deactivation of Fe catalysts by HX poisoning. Co-feeding HX neither significantly changed the distribution of iron carbides (χ-Fe_5C_2 and ε'-$Fe_{2.2}C$) and magnetite nor formed Fe–X compounds. In addition, it was found that Hägg carbide (χ-Fe_5C_2) converted to ε'-$Fe_{2.2}C$ during the startup period or under low temperature FTS conditions. In this study, the poisoning strengths of F^-, Cl^-, and Br^- on the Fe catalyst were also quantified by calculating the loss in surface Fe atoms per halide ion (Fe/X^-), with the following trend being observed at 260 °C: Fe/Br^- (1.0) > Fe/Cl^- (0.9) > Fe/F^- (0.4). This order remained the same at 270 °C, but the Fe/X^- ratio decreased slightly, as expected for an adsorptive mechanism.

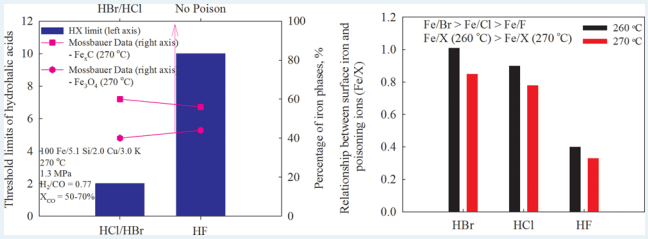

KEYWORDS: *Fischer–Tropsch synthesis, Fe catalyst, poisoning, hydrohalic acids (HX: HF, HCl, or HBr)*

1. INTRODUCTION

As with sulfur compounds (H_2S, COS), halide compounds (NaCl and KCl), NH_3, and hydrohalic acids (HX, X = Cl, Br or F) are also common impurities present in biomass-derived syngas.[1,2] Therefore, investigating the effects of trace amounts of HX poisons on the behavior of Fischer–Tropsch synthesis (FTS) catalysts is important for the development of the biomass-to-liquids (BTL) process. Generally, three main topics are involved in this poisoning investigation: identification of the poisoning limit, measuring the impact of each poison on catalyst performance (e.g., activity, selectivity, and stability), and exploring the mechanism of deactivation. Investigating the influence of catalyst poisons not only aids in the design of better catalysts that are more resistant to the contaminants present in biomass-derived syngas, but defining the thresholds of poisoning levels may also aid in lowering gas purification costs. Few studies to date have reported the impacts of HX impurities on Fe or Co catalyst performance.

The slurry phase reactor is an ideal choice for catalyst sensitivity studies because of its capability of providing a uniform temperature distribution as well as uniform catalyst and poison concentrations in the reactor. Earlier, the effects of sulfur (H_2S, COS),[3,4] halide compounds (NaCl and KCl),[5] and ammonia[3,6,7] on the FTS behavior of Fe and Co catalysts were studied between 220 and 270 °C over long testing periods using a 1 L slurry phase reactor. The Fe-based catalyst was found to be very resistant to ammonia at levels below 200 ppm and to the halide compounds below 40 ppm in syngas;[3,5,7] however, using 400 ppm ammonia in the nitrate form rapidly deactivated the iron catalyst because of oxidation by oxygen-containing nitrogen compound(s) formed from nitrate decomposition.[7] The latter result is important from the standpoint that NO_x may also be present in biomass-derived syngas (e.g., especially from seed corn).[8] Several techniques, such as XRD, Mössbauer spectroscopy, and synchrotron techniques (e.g., XANES, EXAFS) were employed to characterize the used Fe catalysts, to shed light on the nature of the deactivation induced by ammonium nitrate (AN). Results strongly suggested that HNO_3, thermally dissociated from AN, oxidized iron carbides, resulting in a primary route of Fe catalyst deactivation from that poison. A Co catalyst was found to be sensitive to levels even as low as 1.0 ppm ammonia;[6,9] however, the impact of ammonia on catalytic behavior was likely independent of concentration. Co-feeding up to 1200

Received: January 7, 2015
Revised: March 18, 2015
Published: April 8, 2015

ACS Publications © 2015 American Chemical Society

DOI: 10.1021/acscatal.5b00023
ACS Catal. 2015, 5, 3124–3136

ppm ammonia was not found to induce additional deactivation.[6] Recently, the effect of sulfur on Fe and Co catalysts was studied by our group, as well. Both the Fe and Co catalysts tested displayed rapid deactivation in the presence of 0.5 ppm of H_2S.[3,4] The results were consistent with sulfur blocking of active sites as a deactivation mechanism, with each sulfur atom being estimated to eliminate six surface iron or cobalt atoms, on the basis of sorption theory.

In this contribution, the effect of up to 40 ppm of HX in syngas on the performance of a 100 Fe/5.1 Si/2 Cu/3 K catalyst was studied at typical FTS conditions using a 1 L CSTR. HX limits were determined by progressively increasing HX levels, starting from 0.1 ppm. The poison was added only when a steady state was established, such that the deactivation resulting from the added poisons could be measured. XRD and Mössbauer spectroscopy were employed to characterize the used Fe catalysts collected before and after deactivation, with the aim of understanding the deactivation mechanism resulting from HX. The relationship between each halide ion (F^-, Cl^- and Br^-) and resulting losses in surface Fe active sites (e.g., in iron carbides and iron oxides) was determined by assuming that surface Fe species were responsible for FTS and water gas shift (WGS) reactions. HX poisoning resulted in different extents of decreases in the WGS and FTS rates, and this aspect is discussed in terms of the FTS reaction results and characterization data obtained.

Table 1. Results of ICP Analysis of Trace Amounts of Fe and pH Value for the Hydrohalic Acid Solutions and the Water Products Formed in the HX Poisoning Runs

acid solution or FTS water producs	event	Fe concn by ICP, ppm	pH
1700 ppm of HCl	as prepared	0.2	1.47
1700 ppm of HCl	passing through pump and reactor inlet stainless steel tubing	0.9	1.47
2000 ppm of HBr	as prepared	0.7	1.8
2000 ppm of HBr	passing through pump and reactor inlet stainless steel tubing	0.1	1.78
	HCl Test Run		
aqueous sample no. 6 (53 h)	no addition of HCl poison	0.6	n/a
aqueous sample no. 10 (149 h)	testing 1 ppm of HCl in the syngas feed	0.8	n/a
aqueous sample no. 21 (438 h)	testing 10 ppm of HCl in the syngas feed	0.6	n/a
HBr test run			
aqueous sample no. 7 (167 h)	no addition of HBr poison	2.8	n/a
aqueous sample no. 27 (647 h)	testing 0.6 ppm of HBr in the syngas feed	2.4	n/a
aqueous sample no. 49 (1180 h)	testing 20 ppm of HBr in the syngas feed	2.4	n/a

2. EXPERIMENTAL SECTION

2.1. Catalyst Preparation and Characterization. *2.1.1. Preparation of Fe/Si/Cu/K Catalyst.* Details of catalyst preparation can be found elsewhere.[10,11] In brief, a base Fe catalyst 100 Fe/5.1 Si/1.25 K was first prepared using a precipitation method. The 100 Fe/5.1 Si/3.0 K/2.0 Cu catalyst used in this study was prepared by sequential impregnation of an appropriate amount of K- (KNO_3, 99.9% purity) and Cu-($Cu(NO_3)_2{\cdot}2.5\ H_2O$, 99.9% purity) containing solutions. Between steps, the catalyst was dried under vacuum in a rotary evaporator at 80 °C, and the temperature was slowly increased to 95 °C. After the second impregnation/drying step, the catalyst was calcined under air flow at 350 °C for 4 h. The BET surface area, BJH pore volume, and pore diameter were 107 m^2/g, 0.154 cm^3/g-cat, and 6 nm, respectively.[11]

2.1.2. Inductively Coupled Plasma Optical Emission Spectrometry (ICP-OES) Analysis of Impurities in FTS Aqueous Products. To identify whether dilute HX solutions used for the current poisoning study reacted with the pump cylinder and reactor inlet tubing or iron catalyst used (e.g., corrosion), the HCl and HBr solutions with 1700−2000 ppmw (levels similar to those used in the poisoning test runs) were prepared and passed through a high pressure pump and the reactor inlet at a rate of 1.0 mL/h under the reaction pressure (1.3 MPa). The HCl and HBr solution samples, as prepared and collected at the end of the reactor inlet line, together with the water samples produced at different times on-stream in the different HX poisoning test runs, were analyzed by ICP-OES. The ICP results (Table 1) indicate that very small amounts of Fe (0.1−3.0 ppm) were detected in the acid samples and in the FTS water samples, which were within the detection limits of the instrument; moreover, the Fe levels remained virtually unchanged regardless of whether the acid solution passed through the reactor inlet line or was present during FTS. In addition, acidity measurements (Table 1) indicate that the pH values of the acids tested did not change significantly after flowing through the pump and reactor line, which further confirms that no detectable H^+ was lost due to corrosion prior to mixing of the acid solution with the syngas feed. Therefore, the ICP and pH measurements suggest that the corrosive effect of dilute HF, HCl, and HBr solutions on the reactor line or Fe catalyst can be neglected in this study. Finally, the concentration of F^-, Cl^-, or Br^- ions in the prepared acid solutions and in the FTS aqueous products collected at different times were analyzed by ion chromatography (IC) to verify whether there was any uptake of halide by the catalyst.

2.1.3. X-ray Diffraction (XRD) Measurement of Used Fe Catalyst. Powder X-ray diffraction (XRD) was carried out over the used Fe catalysts at room temperature using a Panalytical X'Pert Diffractometer (PW-3040 PRO) operating with Cu Kα radiation (1.5418 Å) to identify Fe carbides/oxides and, potentially, the Fe poison compounds that formed.

2.1.4. Mössbauer Spectroscopy Measurements of the Fe Catalyst. Mössbauer spectroscopy measurements were conducted in transmission mode, with the ^{57}Co source mounted in a standard constant acceleration velocity transducer. The Fe samples in slurry form, which were collected at different times during a run or by the end of a run, were placed in a copper holder and were mounted near the finger of a vibration-free closed-cycle refrigerator, which provided temperatures as low as 20 K. Structural analysis of the samples was performed by least-squares fitting of the Mössbauer spectra to a summation of hyperfine sextets. The least-squares fitting procedure employed user-defined functions within the Peak Fit program. The parameters for each sextet in the fit consisted of the position, width, and height of the first peak, the hyperfine magnetic field, and the quadrupole electric field. These parameters were allowed to vary freely to obtain the best fit of the experimental data. Errors in the determined percentages of Fe values are about ±3% for well-resolved spectra; in those that contain several iron oxide and carbide phases, the uncertainty increases

DOI: 10.1021/acscatal.5b00023
ACS Catal. 2015, 5, 3124−3136

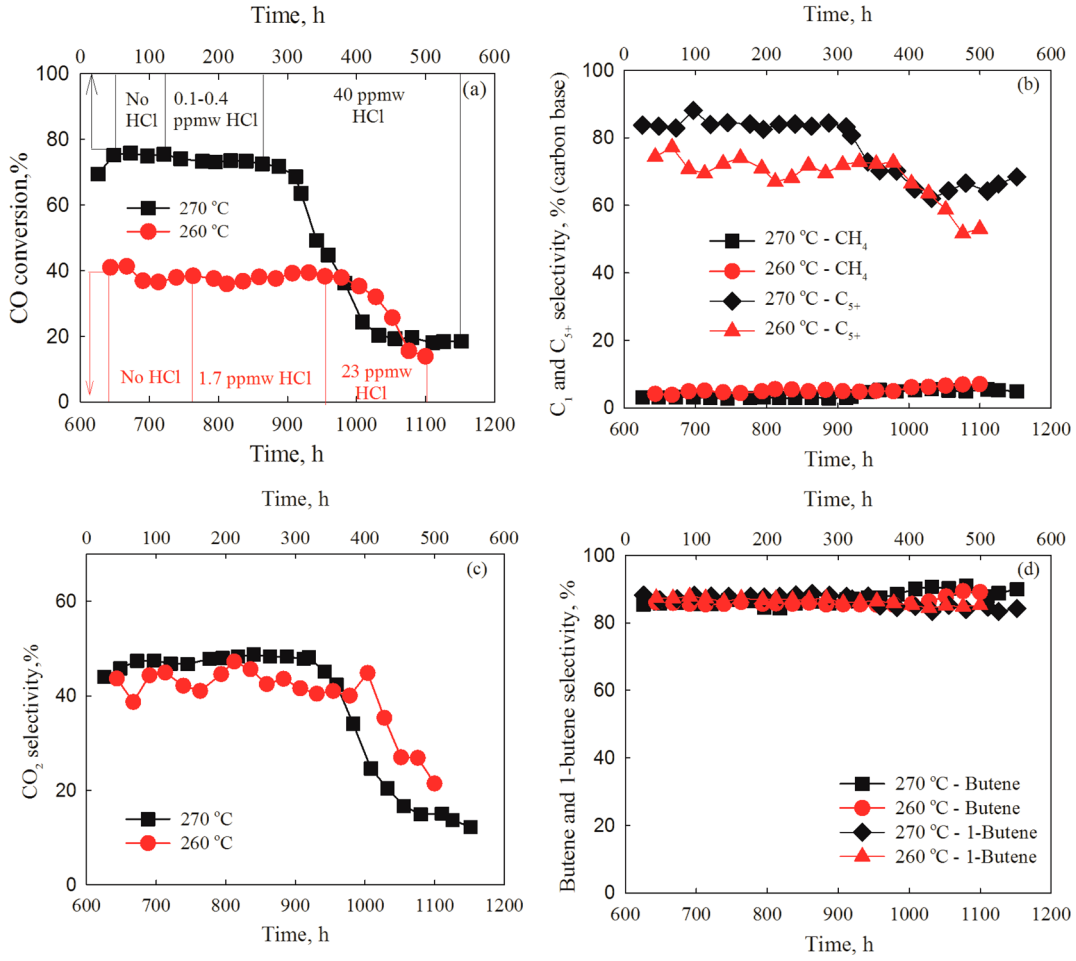

Figure 1. Effect of up to 40 ppm of HCl on (a) CO conversion, (b) CH_4 and C_{5+} selectivities, (c) CO_2 selectivity, and (d) butene and 1-butene selectivities on a 100 Fe/5.1 Si/2 Cu/3 K catalyst under 1.3 MPa (syngas); H_2/CO = 0.67−0.77.

with the complexity of the spectrum (i.e., depending on the degree of overlap and the weakness of the signal).

2.2. Fischer−Tropsch Synthesis Reaction. The 100 Fe/5.1 Si/3.0 K/2.0 Cu catalyst (5−10 g) was activated in situ in a continuously stirred tank reactor (CSTR) using 2 NL/g-cat/h CO at 543.15 K and 1 atm for 24 h. The FTS reaction was carried out under the following conditions: 533−543 K, 10.0 NL/g-cat/h, 1.3 MPa, and H_2/CO ratio of 0.67−0.77. After a steady state was established, usually between 90 and 120 h on-stream, the aqueous impurity-containing solutions (HX) with appropriate concentrations were cofed into the CSTR at 1.0 mL/h using a high performance precision syringe pump (ISCO 500 D). A number of HX levels in the syngas feed, for example, 0.1, 1, 3, 5, 10, 20, 30, and 40 ppm, were examined, and each level was monitored for between 72 and 200 h. Changes in CO conversion, selectivities to CH_4 and C_{5+} (carbon atom basis), CO_2 selectivity, C_4 olefin selectivity (i.e., defined to be 100 × (rate of all C_4 alkenes)/(rate of all C_4 alkenes + rate of all C_4 alkanes)) and 1-C_4 olefin selectivity (i.e., defined to be 100 × (rate of 1-C_4 alkenes)/(rate of all C_4 alkenes)) as functions of time and contaminant concentration were used to evaluate the impacts of each poison.

3. RESULTS AND DISCUSSION

3.1. Effect of HCl on Fe Catalyst Activity and Selectivity. The effect of HCl on Fe catalyst performance was evaluated at 260 and 270 °C in two separate runs after the catalyst reached steady state. At 270 °C, two low HCl levels (100 and 400 ppb) and one high level (40 ppm) were examined between 110 and 550 h (total of 440 h). At 260 °C, after it took a relatively long time to establish a steady state with a CO conversion of 40%, addition of 1.7 and 23 ppm of HCl was examined between 780 and 1100 h (320 h). The effects of different levels of HCl on the Fe catalyst activity, CH_4 and C_{5+} selectivity, CO_2 selectivity, and C_4 olefin and 1-C_4 olefin contents are summarized in Figure 1.

Fe catalyst activity remained relatively unchanged during cofeeding of 100 and 400 ppb levels of HCl between 110 and 280 h. Right after the two low levels were tested, the HCl level was increased significantly to 40 ppm, which is considered to be a high HCl concentration. This led to a rapid CO conversion drop from 73% to 20% in 150 h (280- 430 h, Figure 1a). The CO conversion leveled off in the next 120 h of continuously feeding 40 ppm of HCl. Accompanying the rapid deactivation, CH_4 selectivity increased from 3.0 to 5.3%, and C_{5+} and CO_2 selectivities decreased sharply from 84 to 64% and from 48 to 20%, respectively. (Figure 1b,c). However, the deactivation by HCl did not significantly alter butene and 1-butene selectivities (Figure 1d). Butene and 1-butene selectivities remained relatively constant at between 86 and 87% before and after cofeeding 40 ppm of HCl. Possible reasons that may account for this behavior are discussed in Section 3.4.

At 260 °C, cofeeding a low HCl level of 1.0 ppm for 100 h did not result in significant catalyst deactivation (results not

DOI: 10.1021/acscatal.5b00023
ACS Catal. 2015, 5, 3124−3136

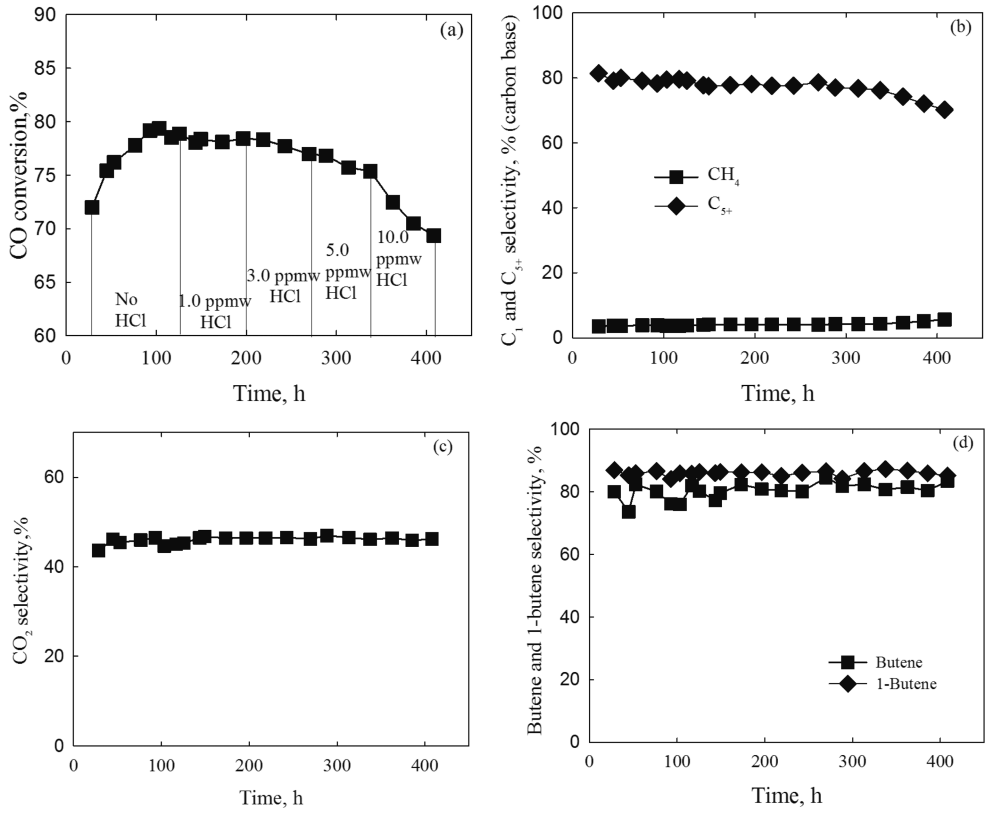

Figure 2. Effect of 1.0−10 ppm of HCl on (a) CO conversion, (b) CH_4 and C_{5+} selectivities, (c) CO_2 selectivity, and (d) butene and 1-butene selectivities on a 100 Fe/5.1 Si/2 Cu/3 K catalyst at 270 °C, 1.3 MPa (syngas); H_2/CO = 0.77.

shown for the sake of brevity). Thereafter, the cofeeding stream of 1.0 ppm of HCl solution was switched off between 643 and 763 h to obtain a new pseudosteady state (Figure 1a). A flat baseline was achieved in this period with a CO conversion of 39%. Subsequently, 1.7 ppm of HCl in the syngas feed was introduced for 191 h (763−954 h), and CO conversion remained relatively stable. However, when the HCl level was increased to 23 ppm, the activity declined linearly over the next 153 h, and then it leveled off at 16% CO conversion between 1075 and 1100 h. This result is rather similar to the phenomena observed in the latter period of testing 40 ppm of HCl at 270 °C. The result suggests that HCl poisoning of the Fe catalyst was through an adsorption process. A significant impact of HCl on the adsorption of CO, H_2 and intermediates on the catalyst surface appears to occur at a certain conversion level, that is, above 20%, and thereafter reaches a state of saturation on the Fe active sites. The trends in Fe catalyst selectivities with addition of low or high levels of HCl at 260 °C are similar to those obtained at 270 °C. Large increases in CH_4 selectivity and decreases in C_{5+} and CO_2 selectivities were observed only after the high level of HCl (i.e., 23 ppm) was used beginning at 950 h of time on-stream.

One of the main objectives of this study was to determine the threshold limit of HX to provide valuable information regarding the degree of syngas purification required. To that end, a run was conducted at 270 °C with the aim of quantifying the HCl limit for the catalyst. Additional HCl concentrations (i.e., 1, 3, 5, and 10 ppm) were examined, and each level was tested over a time period of 70−96 h, as shown in Figure 2a−d. The cofeeding of 1.0 ppm of HCl for 96 h did not significantly affect CO conversion (78.2%), in agreement with the trend obtained at 260 °C. When the HCl level was increased to 3.0 ppm at 200 h, a measurable deactivation was observed, and CO conversion started to decrease slowly from 78.2 to 76.9% within 72 h. However, as the HCl level was progressively increased to 5.0 and 10.0 ppm at 270 and 338 h, respectively, more rapid declines in catalyst activity were observed. The deactivation rate (i.e., defined as the percentage decrease in CO conversion per day) increased from 0.61%/day to 0.74%/day and further to 2.7%/day when the HCl level was changed from 3 to 5, and further to 10 ppm. Therefore, by combining the results shown in Figures 1 and 2, the conclusion is drawn that ∼2 ppm of HCl in the syngas feed is a problem for the Fe catalyst tested. The effects of addition of 1.0, 3.0, 5.0, and 10.0 ppm of HCl on Fe catalyst selectivities are shown in Figure 2b−d. CH_4 selectivity and C_{5+} selectivity were more or less stable between 125 and 338 h (i.e., where concentrations ranging from 1.0 to 5.0 ppm of HCl were examined); however, a slight increase in CH_4 selectivity accompanied by a slight decrease in C_{5+} selectivity occurred when the addition of 10 ppm of HCl was commenced at 338 h. It is interesting that adding up to 10 ppm of HCl for 283 h did not significantly alter CO_2 and butane selectivities. These selectivity trends are in good agreement with the results obtained in the first two HCl runs, as shown in Figure 1b−d.

3.2. Effect of HBr on Fe Catalyst Activity and Selectivity. An assessment of the effects of various levels of HBr in the syngas feed was also performed at 260 and 270 °C in separate runs. Identical levels used in the first HCl test run (i.e., conducted at 270 °C and using 100 and 400 ppb and 40 ppm of HBr) were examined at 270 °C for 200 h. At 260 °C, a low level (0.6 ppm), a moderate level (5.0 ppm) and a high level (20.0 ppm) were examined. Each level was tested under FTS conditions for more than 120 h. The effects of up to 40

DOI: 10.1021/acscatal.5b00023
ACS Catal. 2015, 5, 3124−3136

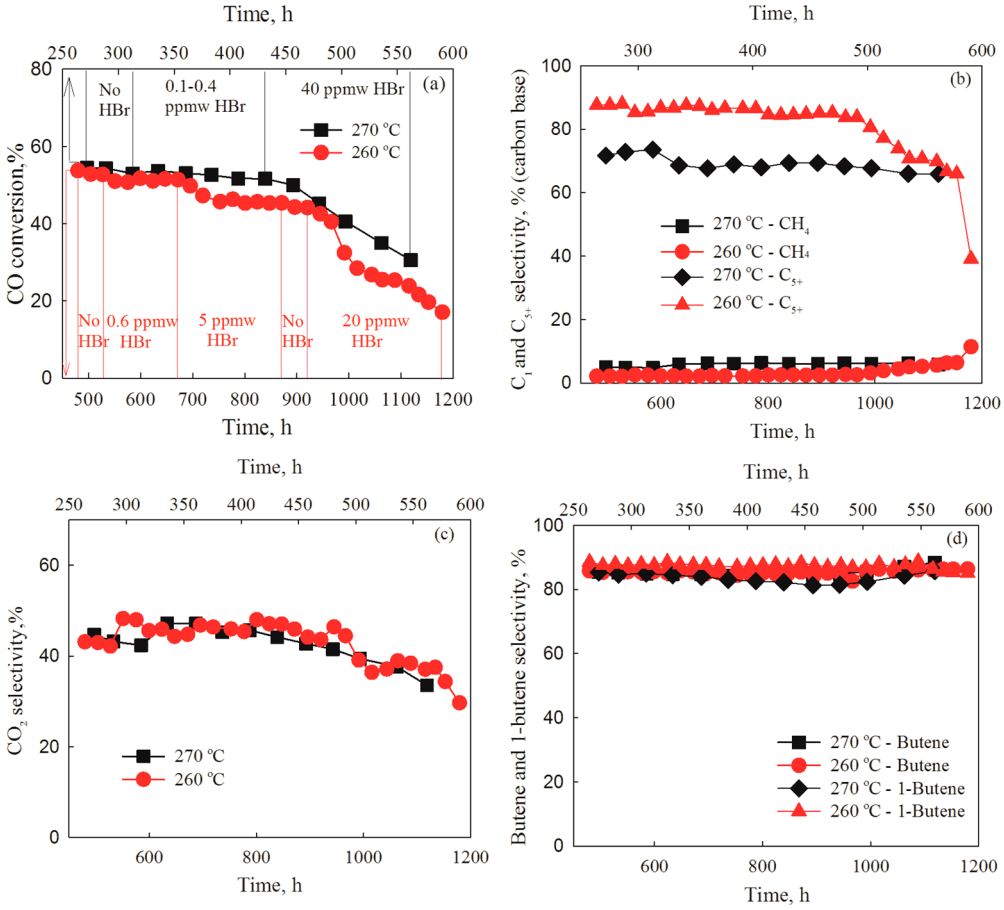

Figure 3. Effect of up to 40 ppm of HBr on (a) CO conversion, (b) CH_4 and C_{5+} selectivities, (c) CO_2 selectivity, and (d) butene and 1-butene selectivities on a 100 Fe/5.1 Si/2 Cu/3 K catalyst under 1.3 MPa (syngas); H_2/CO = 0.67−0.77.

ppm of HBr on the Fe catalyst activity and product selectivities are illustrated in Figure 3a−d.

At 270 °C, a first attempt to cofeed HBr solution to give 100−400 ppb levels triggered Fe catalyst deactivation, and CO conversion decreased rapidly from 73 to 54% within 150 h (121−271 h, Figure 3); however, a baseline CO conversion of ∼54% was achieved after cofeeding of 100 ppb HBr was suspended between 271 and 312 h. On the basis of this new established steady state, concentrations in the range of 100−400 ppb HBr were retested in the time period of 313−432 h, followed by the examination of a high HBr level (i.e., 40 ppm, between 432 and 562 h), as shown in Figure 3. Apparently, the Fe catalyst was nearly stable during feeding of 100−400 ppb for 119 h, and this in turn demonstrated that the deactivation observed during the first cofeeding test of 100−400 ppb HBr was likely not the result of the low levels of HBr. On the other hand, 40 ppm of HBr was a high enough level to cause rapid deactivation of the Fe catalyst; for example, a marked CO conversion drop from 52 to 30.6% was observed in 130 h of testing. In line with the results obtained in the HCl run, decreases in C_{5+} selectivities and CO_2 selectivity were observed, when adding 40 ppm of HBr, but to a lesser extent. Again, selectivities of butane and 1-butene maintained high values (i.e., 84%) without changing significantly during the HBr cofeeding tests.

At 260 °C, after a pseudosteady state was established, a low level of 0.6 ppm of HBr was first tested between 527 and 671 h without greatly affecting CO conversion (∼51%). Continuous examination of the effects of a moderate HBr level of 5 ppm on catalyst performance was then carried out for 200 h, and slow deactivation was observed. CO conversion decreased 6% (51.4 → 45.4%) in the test period (Figure 3a). The run was conducted without adding contaminant-containing solution between 871 and 920 h to achieve a pseudosteady state and verify the intrinsic catalyst deactivation rate. In the scenario of increasing the HBr level to 20 ppm starting from 920 h, rapid deactivation of the Fe catalyst occurred. CO conversion decreased from 45 to 17% in 260 h (Figure 3a, 920−1180 h), which was similar to the trend observed in Figure 1a for the testing of 23 ppm of HCl. Accompanying this rapid deactivation, significant changes in the C_1 (increase), C_{5+}, and CO_2 selectivities (decreases) were observed (Figure 3b,c); however, C_4 olefin and 1-C_4 olefin selectivity remained nearly constant before and after the addition of HBr, in line with the results at 270 °C for the HCl run. A conservative threshold limit for HBr for this catalyst is 1 ppm as, at a level of 5 ppm, slow deactivation was observed, although selectivities were not significantly impacted. However, 20 ppm of HBr or above rapidly deactivated the Fe catalyst and adversely shifted selectivity toward lighter hydrocarbons and decreased CO_2 selectivity. In short, the deactivation caused by HBr on the Fe catalyst was quite similar to that of HCl and may be explained by an adsorption mechanism (i.e., site blocking), to be discussed in Section 3.5.

3.3. Effect of HF on Fe Catalyst Activity and Selectivity. The effects of different levels of HF on the Fe

DOI: 10.1021/acscatal.5b00023
ACS Catal. 2015, 5, 3124−3136

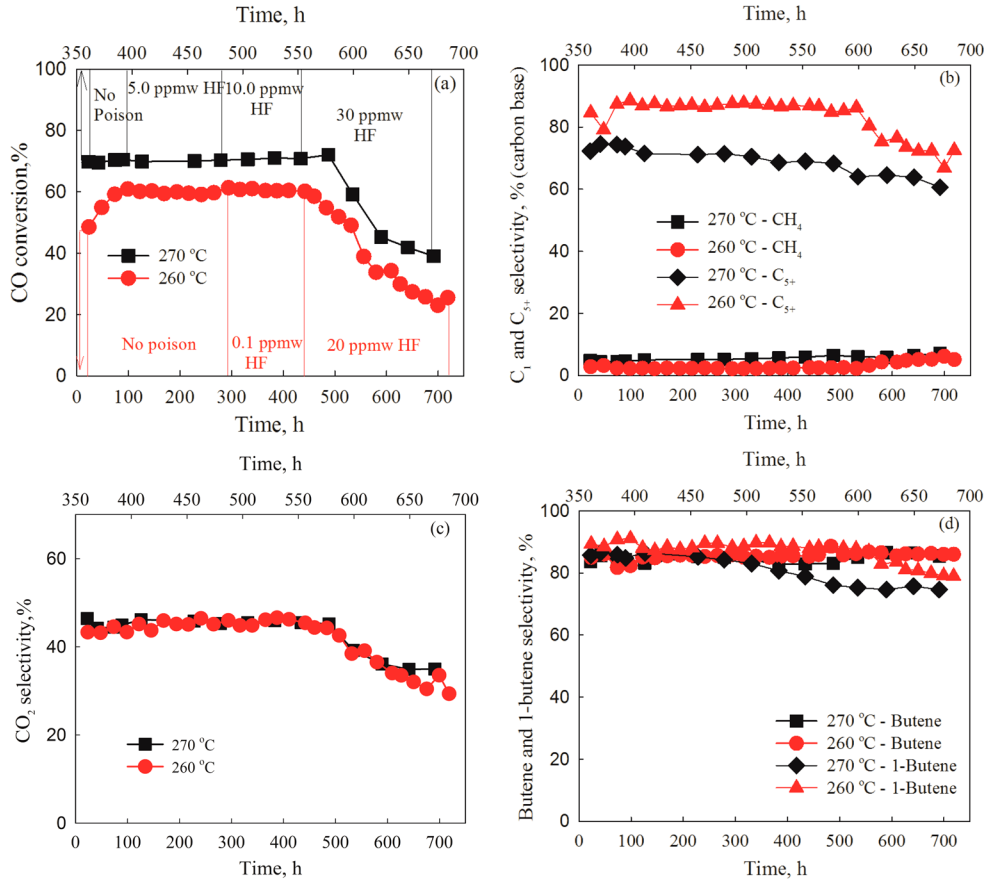

Figure 4. Effect of up to 30 ppm of HF on (a) CO conversion, (b) CH_4 and C_{5+} selectivities, (c) CO_2 selectivity, and (d) butene and 1-butene selectivities on a 100 Fe/5.1 Si/2 Cu/3 K catalyst under 1.3 MPa (syngas); H_2/CO = 0.67−0.77.

Table 2. Results of Mössbauer Spectroscopy Least-Squares Fitting of the Fe Catalysts before and after Co-Feeding Hydrohalic Acids[a]

	iron phases			details of iron carbides						
poison/ TOS, h	Fe % in magnetite	Fe % in carbides	Fe %	Fe % in G1	Fe % in B1	Fe % in B2	Fe % in G2	Fe % in B3	G1 + G2 (ε'-$Fe_{2.2}C$)	summary of iron carbides B1 + B2 + B3 (χ-Fe_5C_2)
after reduction/0	19.0	81.0	0.0	5.0	28.0	28.0	2.0	18.0	7.0	74.0
no poison/78	44.0	56.0	0.0	4.0	17.0	17.0	3.0	14.0	7.0	48.0
HCl, 270 °C/ 552	35.0	65.0	0.0	13.0	13.0	9.0	16.0	14.0	29.0	36.0
HBr, 270 °C/ 648	40.0	60.0	0.0	8.0	16.0	10.0	13.0	13.0	21.0	39.0
HF, 260 °C/ 817	31.0	61.0	8.0	12.0	7.0	5.0	29.0	8.0	41.0	20.0
HCl, 260 °C/ 1146	25.0	75.0	0.0	19.0	11.0	4.0	32.0	9.0	51.0	24.0
HBr, 260 °C/ 1223	20.0	80.0	0.0	21.0	12.0	4.0	31.0	12.0	52.0	28.0

[a]G1 and G2 stand for the green sextets in Figures 8 and 9; B1, B2, and B3 stand for the blue signals in Figures 7 and 8).

catalyst were examined at 260 and 270 °C. Figure 4a−d presents the changes in CO conversion, CH_4 and C_{5+} selectivities, CO_2 selectivity, and butene and 1- butene contents with time and HF level. At 270 °C, a pseudosteady state was established at 70% CO conversion between 360 and 392 h. Thereafter, 5, 10, and 30 ppm levels of HF were tested in the time periods of 392−480 (88 h), 480−553 (73 h), and 553−673 h (100 h), respectively. Interestingly, CO conversion remained relatively constant at ∼70% during cofeeding of 5.0−10 ppm of HF for 161 h. In contrast, catalyst activity started to decline sharply after a 30 ppm level of HF was introduced. The results indicate that the HF threshold limit for this Fe catalyst (i.e., 10 ppm) is higher than that of either HCl or HBr (i.e., 1−2 ppm), in line with a much lower Fe/X^- ratio determined for the case of F^-, as described in Section 3.7.

From Figure 4, CO conversion stabilized at 60% at 260 °C during the period of 73−265 h. Cofeeding 0.1 ppm of HF in the syngas was performed over the next 145 h, and it did not measurably alter the catalyst activity and selectivities; however, cofeeding a high level of HF, 20 ppm, for another 289 h caused

DOI: 10.1021/acscatal.5b00023
ACS Catal. 2015, 5, 3124−3136

a rapid decline in activity and changed the hydrocarbon and CO_2 selectivities without significantly altering C_4 olefin contents. (Figure 4b–d). By the end of the run at 710 h, only 23% CO conversion remained. Thus, the results at 260 °C further confirmed that HX concentrations at or exceeding 20 ppm were sufficiently high to induce sharp activity losses in the Fe catalyst.

3.4. Selectivity Trends Observed during HX Poisoning of the Fe Catalyst. The present study consistently revealed that adding a high level of HX poison (i.e., ≥20 ppm) resulted in significant decreases in C_{5+} and CO_2 selectivities, while C_4 olefin and 1-C_4 olefin (or 2-C_4 olefin) remained relatively unchanged. The overall amounts of iron carbides and magnetite, as discussed in Section 3.5 to follow, did not significantly change (Table 2), which indicates that the selectivity trends observed after exposing the catalyst to high levels of HX for several days are not due to changes in bulk catalyst structure. Since the effect of CO conversion level (<70%) does not significantly affect hydrocarbon selectivity for iron-based catalysts,[12,13] the changes in the selectivities are assumed to be mainly associated with the impact of HX on adsorption of reactants, desorption of products, or both. Presumably, halide ions adsorbed on iron catalyst active sites and promoted chain termination or suppressed chain propagation, resulting in decreases in C_{5+} selectivity and CO_2 selectivity. In this context, the adsorbed halide ions appear to more strongly inhibit CO adsorption than H_2 during the periods of deactivation.

As shown in Figure 5, the deactivation resulting from cofeeding of HX led to significantly higher partial pressures of

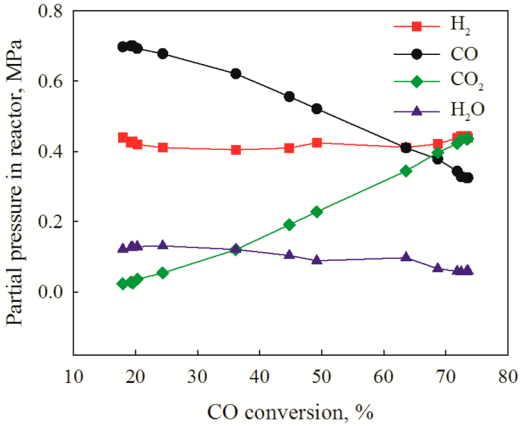

Figure 5. Change of partial pressures of H_2 and CO during deactivation by cofeeding 40 ppm of HCl over a 100 Fe/5.1 Si/2 Cu/3 K catalyst at 270 °C, H_2/CO feed ratio = 0.77, and 1.3 MPa.

CO, (0.32 → 0.76 MPa when X_{CO} decreased from 75 to 15%) and presumably higher CO surface fugacities on the catalyst surface (noting that CO is a reactant for both WGS and FTS). On the other hand, the partial pressure of H_2 remained nearly unchanged (~0.46 MPa). For the case of biomass-derived syngas having a low H_2/CO ratio, to achieve high CO conversion, WGS is required to supply the H_2 needed for the FTS reaction, and CO_2 provides an indicator of the extent of WGS. Adding HX may significantly reduce the formation of hydrocarbon intermediates, C_nH_{2n+1}–S, and, consequently, suppress the formation of long chain hydrocarbons. This assumption may also explain the nearly unchanged C_4 olefin and 1-C_4/2-C_4 olefin selectivities observed during the periods of significant deactivation resulting from HX poisoning; it is widely viewed that hydrocarbon intermediates, C_nH_{2n+1}–S, will be either dehydrogenated or hydrogenated to form olefins or paraffins, respectively, in the termination step. Moreover, hydrogenation of 1-olefin to paraffin, or readsorption and isomerization of 1-olefins to internal olefins may also occur. If one assumes that HX does not affect CO adsorption on the Fe catalyst, an increase in C_4 olefin selectivity with severe deactivation due to the partial pressure of CO adversely affecting 2-C_4 formation[14,15] would be expected. Another reason for the observed constant olefin and 1-, 2-olefin contents should be attributed to the relatively unchanged partial pressure of H_2, which would tend to maintain the hydrogenation rate or isomerization rate relatively constant.

3.5. Deactivation Mechanism of the Fe Catalysts by HX. The Fe catalyst displayed rapid deactivation regardless of the conditions used when the level of hydrohalic acid reached 20+ ppm. Two possible mechanisms could be responsible for the observed deactivation. One is physical blocking of active sites by halide ions (i.e., F^-, Cl^-, or Br^-) due to the adsorption of ions on the Fe catalyst surface; another potential pathway is the formation of iron halide (Fe-X) compounds. To verify the mechanisms proposed, the Fe phases of the Fe catalysts after reduction, as well as before and after HX poisoning, were analyzed by XRD and Mössbauer spectroscopy. Figure 6a,b and Figures 7 and 8 present the results of XRD and Mössbauer spectroscopy of the Fe catalysts, respectively.

The XRD profiles of the used Fe catalysts either under clean conditions or after poisoning (i.e., after examining up to 40 ppm of HCl or HBr) at 270 °C display similar XRD line patterns in the 2θ range of 20–80° (Figure 6a). The most intense reflections observed are located at 2θ values of 35.5° and 40°, 42.6°, 45.0°, which represent the characteristic peaks of Fe_3O_4 and Fe_5C_2, respectively, and they are present in all three used Fe samples. The nearly unchanged intensities and locations of the Fe_3O_4 and Fe_5C_2 peaks in the three spectra likely suggest that online addition of HX poison did not result in Fe phase transformation or the generation of new Fe-X phases with sufficient long-range order to be detected by XRD. Furthermore, the XRD results of the HF-, HCl-, and HBr-poisoned samples after testing at 260 °C (Figure 6b) are consistent with this conclusion, as the characteristic peaks of Fe_3O_4 and Fe_5C_2 phases present at 260 °C also remained relatively unchanged among the three samples tested for each hydrohalic acid. Thus, the results are in line with a site blocking mechanism for HX.

However, comparing the XRD patterns for the different temperatures (i.e., comparing Figure 6a and b), some differences are observed. The intensities of the Fe_5C_2 peaks in all samples tested at 260 °C are higher than those tested at 270 °C, and the trend for the Fe_3O_4 peaks at the two temperatures exhibit the opposite trend. The XRD results further indicate that additional iron carbides, and with larger relative cluster size, along with correspondingly less magnetite, were formed at 260 °C, consistent with the results of Mössbauer spectroscopy as discussed below.

The Mössbauer spectra of the used samples tested at 270 °C and collected before FTS (0 h), after reaching steady state (78 h) or at the end of the HCl or HBr cofeeding runs, are shown in Figure 7a–d; the Mössbauer spectra of the used samples tested at 260 °C (and collected at the end of HF, HCl, or HBr cofeeding runs) are shown in Figure 8a–c. The results of Mössbauer spectroscopy by least-squares fitting of Fe catalysts

DOI: 10.1021/acscatal.5b00023
ACS Catal. 2015, 5, 3124–3136

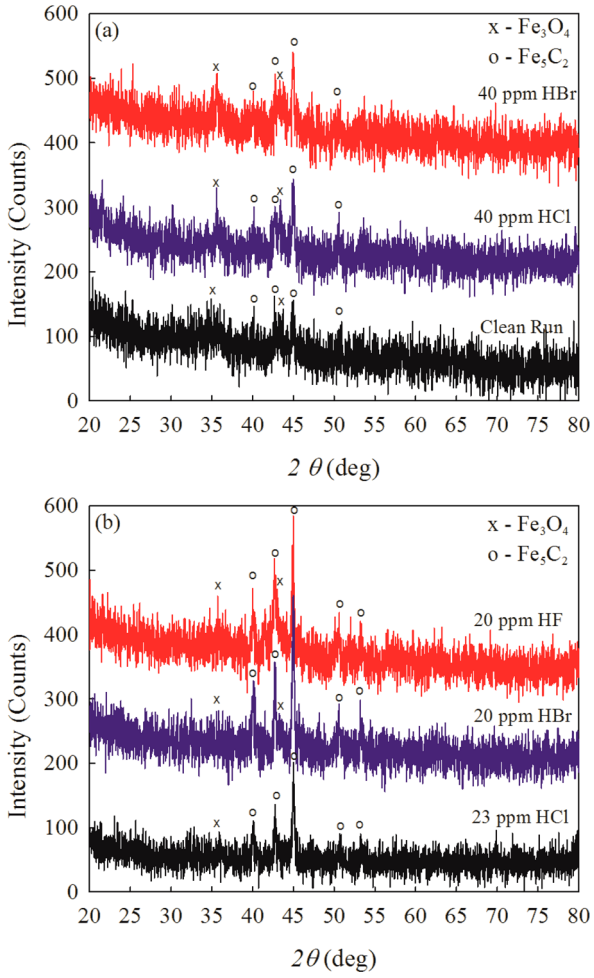

Figure 6. XRD spectra of the used 100 Fe/5.1 Si/2 Cu/3 K catalyst tested at (a) 270 and (b) 260 °C.

are summarized in Table 2. Three phases of iron (i.e., χ-Fe_5C_2, ε'-carbide, and magnetite (Fe_3O_4)) are identified in all samples, which are represented by three blue sextets, two green sextets, and one red sextet, respectively. The spectra of the used samples collected at different times on-stream changed significantly (Figure 7a–d); however, the spectra of the used samples for all three types of hydrohalic acids were very similar (Figure 7c,d and Figure 8a–c). After CO pretreatment, the Mössbauer spectrum displayed enhanced blue sextets and relatively small green sextets and red sextet (Figure 7a); this indicates that a significant amount of χ-Fe_5C_2 was formed, accompanied by a small amount of ε'-carbide and magnetite. This is confirmed by the fitting results showing the catalyst after CO reduction consisting of 74% χ-Fe_5C_2, 7% ε'-carbide, and 19% Fe_3O_4 (Table 2). When the Fe catalyst was exposed to FTS for 78 h, where a steady state was established, the blue sextets slightly decreased, but the red sextet increased in intensity; on the other hand, the green sextets remained relatively unchanged. Table 2 shows that the amount of χ-Fe_5C_2 decreased to 48%, and that of magnetite increased to 44% during the first 78 h of FTS reaction; moreover, the amount of ε'-carbide remained at 7%. The results demonstrate that the Fe catalyst experienced a phase transformation during the startup period, with 35% of χ-Fe_5C_2 being converted to Fe_3O_4. The formation of water during FTS has been reported to be the major reason for the conversion of iron carbides to magnetite.[16]

After examining 40 ppm of HCl or 40 ppm of HBr for several hundreds of hours at 270 °C, the blue sextets continued to decrease, the green sextets started to increase, and the red sextets remained nearly unchanged in both cases. Table 2 indicates that, by the end of HCl and HBr test runs, the amount of χ-Fe_5C_2 in the catalyst decreased to 36–39%, and the amount of ε'-carbide increased to 21–29%, making the total amount of iron carbides both before and after HX poisoning at 270 °C remarkably similar (56–64%). Meanwhile, the amount of Fe_3O_4 remained in the range of 35–40% after testing HX, close to the value prior to the introduction of HX. These results suggest that oxidation of iron carbides did not occur to a significant extent during poisoning, and neither were FeX compounds formed to a significant extent. HX adsorption with blocking of active sites was most likely the primary route of catalyst deactivation. Note that ε'-$Fe_{2.2}C$ in the Fe catalyst after testing HCl or HBr at 270 °C increased, which was different from the results reported in the study of ammonia compounds,[7] where the ε'-$Fe_{2.2}C$ amount was less changed (7–11%). This could be due to the oxidizing environment present in the AN cofeeding run, with oxidation of iron carbides proceeding much faster than the Fe phase transformation.

Turning to the Mössbauer spectra of the used Fe catalyst tested at 260 °C (Figure 8 and Table 2), all three Mössbauer spectra of the used catalysts after exposure to HF, HCl, or HBr displayed patterns similar to the results obtained at 270 °C. The three Fe catalysts contained similar percentages of Fe phases (i.e., 70–80% iron carbides and 20–30% magnetite). These numbers are close to the Fe phase composition after CO carburization (i.e., activation), but different from that of the Fe samples tested at 270 °C. Thus, the discrepancy in data between the two temperature conditions revealed by the Mössbauer spectroscopy data is consistent with the results of XRD shown in Figure 6. However, note that the distribution of the two iron carbides at 260 °C changed considerably. Approximately 67% of Fe carbides were ε'-carbide, with the remainder being identified as χ-Fe_5C_2. The increase in ε'-$Fe_{2.2}C$ suggests that a fraction of χ-Fe_5C_2 was not sufficiently stable under the low temperature conditions and converted to ε'-$Fe_{2.2}C$ during FTS.

In brief, both the results from XRD and Mössbauer spectroscopy suggest that the deactivation of the Fe catalyst by HX was through adsorption and site blocking by halide ions as the primary deactivation mechanism. This is consistent with the leveling off in FTS activity observed during testing of the high levels of HX (20–40 ppm) at different temperatures.

There have been few studies to date on the effect of HX on Fe catalyst performance. van Steen et al.[1] reported that HX may interact with the irreducible oxides in the catalyst, resulting in creep of the support material, consequently deactivating the FTS catalyst. Borg et al.[17] studied the effect of 0–1000 ppmw alkali (Na^+ and K^+) and alkaline earth metals (Ca^{2+} and Mg^{2+}) and Cl^- on cobalt catalyst performance by preadding these biomass-derived syngas impurities to the catalyst surface. The presence of 800–1300 ppm of Cl^- was not found to affect cobalt catalyst performance but increased C_{5+} selectivity, whereas an electronic effect from Ca^{2+} or Mg^{2+} was postulated to explain the resulting deactivation. Hofer[18] studied the reaction of iron carbide with acid in solution and found that iron carbides can react readily with acids to form hydrocarbons, free carbon, and ferrous iron in solution. This could occur through deterioration and hydrolysis processes, depending on the acidity of the solution and inhibition by reaction products.

DOI: 10.1021/acscatal.5b00023
ACS Catal. 2015, 5, 3124–3136

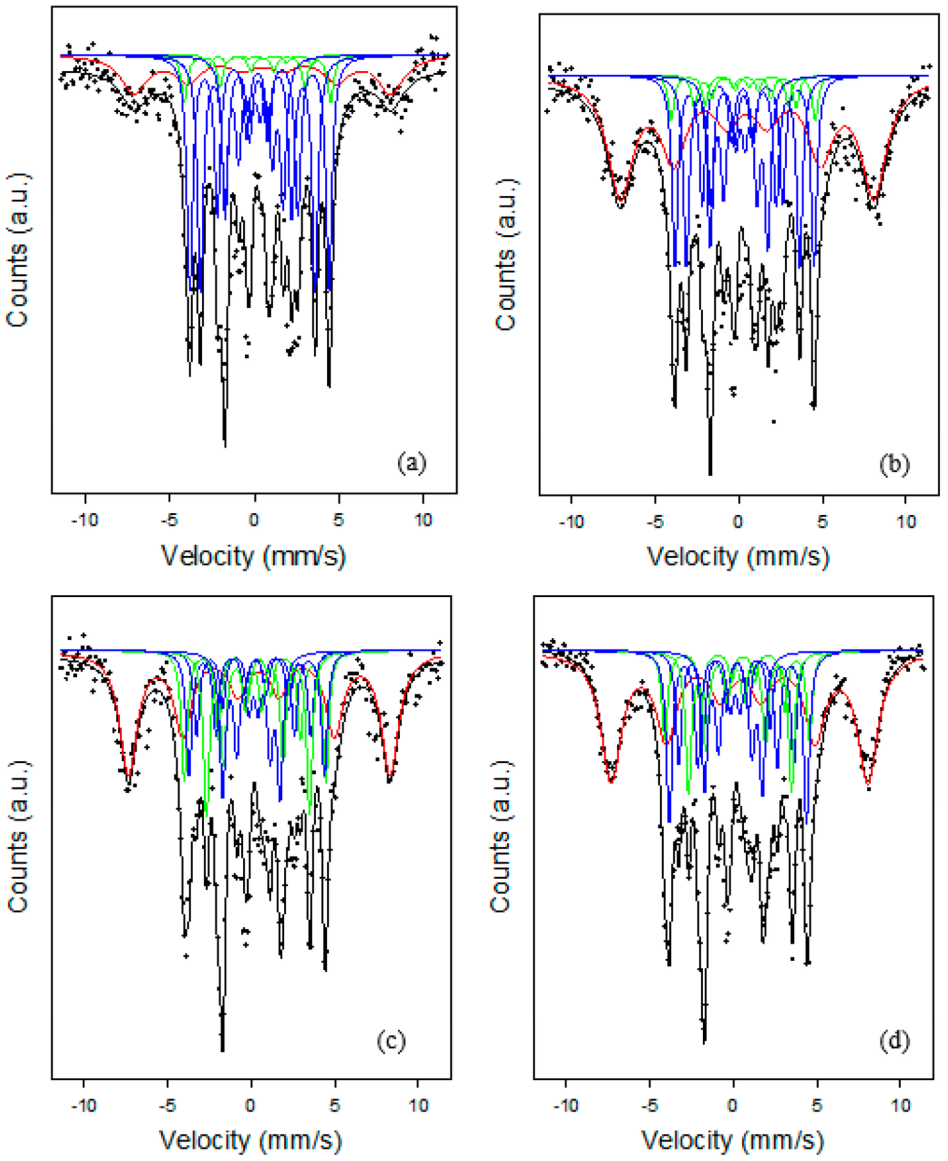

Figure 7. Mössbauer spectra of the 100 Fe/5.1 Si/2 Cu/3 K catalyst tested at 270 °C (a) after reduction (i.e., time on-stream = 0 h), (b) before poisoning (78 h), (c) after HCl poisoning (552 h), and (d) after HBr poisoning (648 h). Blue sextets = Hägg's carbide; green sextet G2 = $\acute{\epsilon}$-$Fe_{2.2}C$; and red sextets = magnetite.

The conditions used in the present work were a high temperature and high pressure, with trace amounts of HX impurities being cofed online, and they should be in the vapor phase and gradually diffuse through the liquid layer to the catalyst surface to cause deactivation. Therefore, neither deterioration and hydrolysis nor creep are likely routes of deactivation in the current context. Electronic effects of the halide ions on catalyst performance could not be ruled out, but further study is required to clarify this issue.

3.6. IC Analysis Results of Hydrohalic Acid Solutions and FTS Aqueous Products. The concentrations of halide ions in three prepared hydrohalic acid solutions (HX) and in the FTS water products collected during testing with the addition of 20−40 ppm of HX (high enough to deactivate the Fe catalyst) in the syngas feed are shown in Tables 3 and 4. The data in Table 3 indicate that IC analyses of F^-, Cl^-, and Br^- ions in the aqueous phase are sufficiently accurate, with the concentrations of F^-, Cl^-, and Br^- ions in the corresponding acid feed solutions (1970, 1344, and 1512 ppm) determined by the IC technique being quite close to the expected values (1920, 1244, and 1244 ppm). The data in Table 4 show that the concentrations of halide ions in the water samples collected between 380 and 560 h in all three poisoning runs are consistent and relatively low (e.g., 1−36 ppm). This indicates that only between 1 and 6% of halide ions exited the reactor, whereas the majority of ions were retained in the reactor and participated in adsorption. (Figure 9). The IC results are in line with an adsorptive mechanism for HX, consistent with the XRD and Mössbauer spectroscopy results discussed previously in Sections 3.4 and 3.5. In short, it is reasonable to assume that all introduced halide ions were taken up by the Fe catalyst for the purpose of discussion of the Fe/X relationship in the following section.

3.7. Determination of the Relationship between Surface Iron and Halide Ions (Fe/X^-). Because an adsorptive (e.g., site-blocking) deactivation mechanism was proposed for HX poisoning of the Fe catalyst, it is important to determine how much each halide ion, on average, was responsible for

DOI: 10.1021/acscatal.5b00023
ACS Catal. 2015, 5, 3124−3136

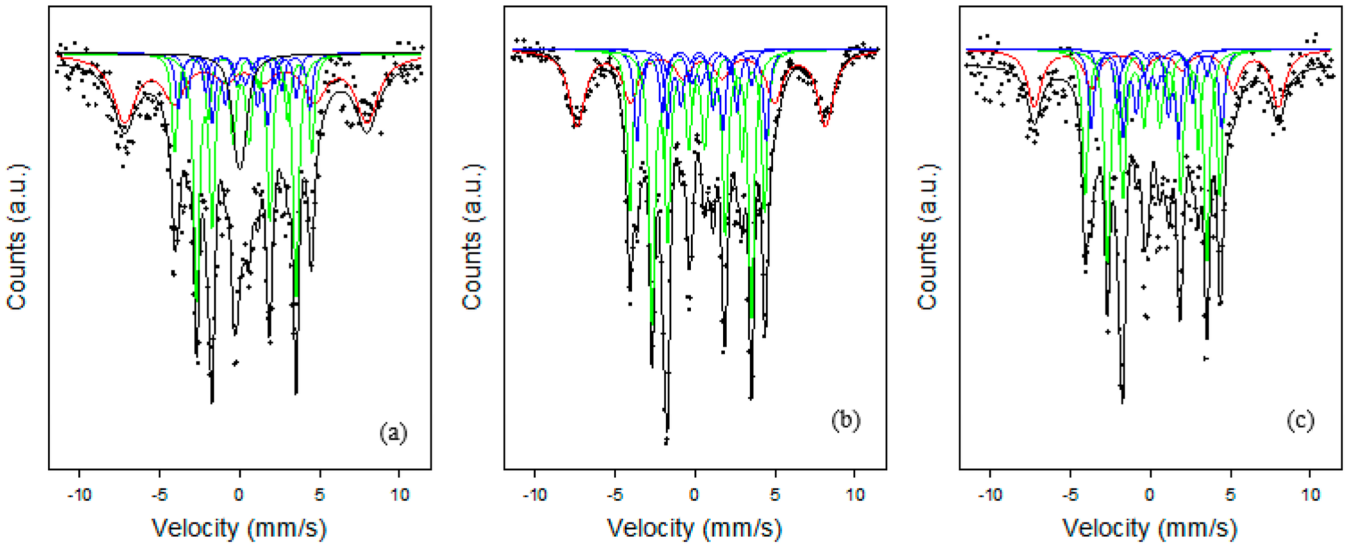

Figure 8. Mössbauer spectra of the 100 Fe/5.1 Si/2 Cu/3 K catalyst tested at 260 °C (a) after HF poisoning (817 h), (b) after HCl poisoning (1146 h), and (c) after HBr poisoning (1223 h). Blue sextets = Hägg's carbide; green sextet G2 = $\acute{\epsilon}$-$Fe_{2.2}C$; and red sextets = magnetite.

Table 3. IC Results for F, Cl, or Br Concentrations in Hydrohalic Acid Solutions

hydrohalic acid (HX) solution prepared for the poisoning test	IC result of F^-, Cl^-, or Br^- ion level in HX solution, ppm	
	expected value	actual value
HF	1920	1970
HCI	1244	1344
HBr	1244	1512

losses in surface iron atoms. In this way, the poisoning strength of different halide ions could be assessed. Accordingly, the relationship between losses in surface iron atoms and halide ions introduced (Fe/X^-) was studied for each hydrohalic acid. Fe and X^- show good linear relationships for all halide ions tested and at different conditions; this, in turn, gives credence to the proposed adsorption mechanism as the predominant reason for catalyst deactivation by HX poisoning.

To calculate the Fe/X^- ratio, surface active sites of the iron phases are assumed to be responsible for the FTS and WGS reactions. Thus, the percentage of losses in surface Fe sites must be proportional to the percentage of CO rate decrease. The number of surface iron atoms per unit catalyst was estimated using the catalyst surface area and the Fe catalyst density of 9.4×10^{-20} m^2/Fe.[19] On the basis of this principle,

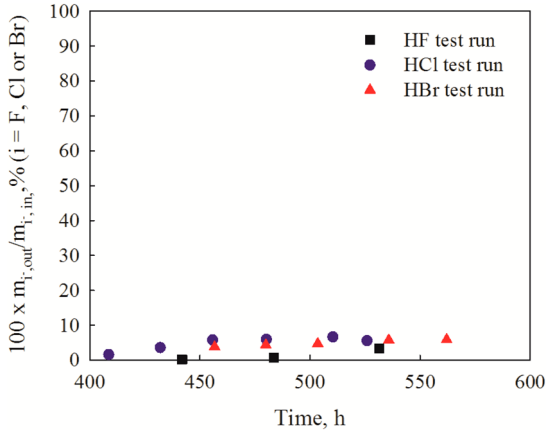

Figure 9. Change in percentage of F^-, Cl^-, and Br^- ions exiting the reactor with time in different poison test runs (ICP analysis results).

the total amount of HX poison fed and corresponding total loss in surface Fe atoms based on CO rate during cofeeding of HX could be obtained. Considering that larger experimental errors can occur when using lower poison concentrations, only the HX levels of 20 ppm or above and their resulting pronounced deactivation rates were used to determine the Fe and halide ion relationship. This error could be minimized and, thus, the Fe/X^- ratios obtained were more accurate. The changes in

Table 4. IC Results of F^-,Cl^- or Br^- Ions in FTS Aqueous Products Formed in Different Poisoning Runs Using 100 Fe/5.1 Si/2 Cu/3 K

HF test run at 260 °C (30 ppm of HF in the syngas feed)			HCl test run at 270 °C (40 ppm of HCl in the syngas feed)			HBr test run at 270 °C (40 ppm of HBr in the syngas feed)		
sample	time, h	F^- level, ppm	sample	time, h	Cl^- level, ppm	sample	time, h	Br^- level, ppm
1	441.9	2	1	382.9	9.7	1	456.7	29.7
2	483.5	5	2	408.6	7.2	2	479.9	31.1
3	531.4	19	3	432.0	15.9	3	503.5	29.7
			4	455.8	26	4	535.8	31.8
			5	480.2	35.7	5	562.1	30.8
			6	510.4	30.4			
			7	525.9	26.1			

DOI: 10.1021/acscatal.5b00023
ACS Catal. 2015, 5, 3124−3136

estimated surface iron lost with the amounts of HF, HCl, and HBr introduced at 270 and 260 °C are shown in Figure 10a and b, respectively.

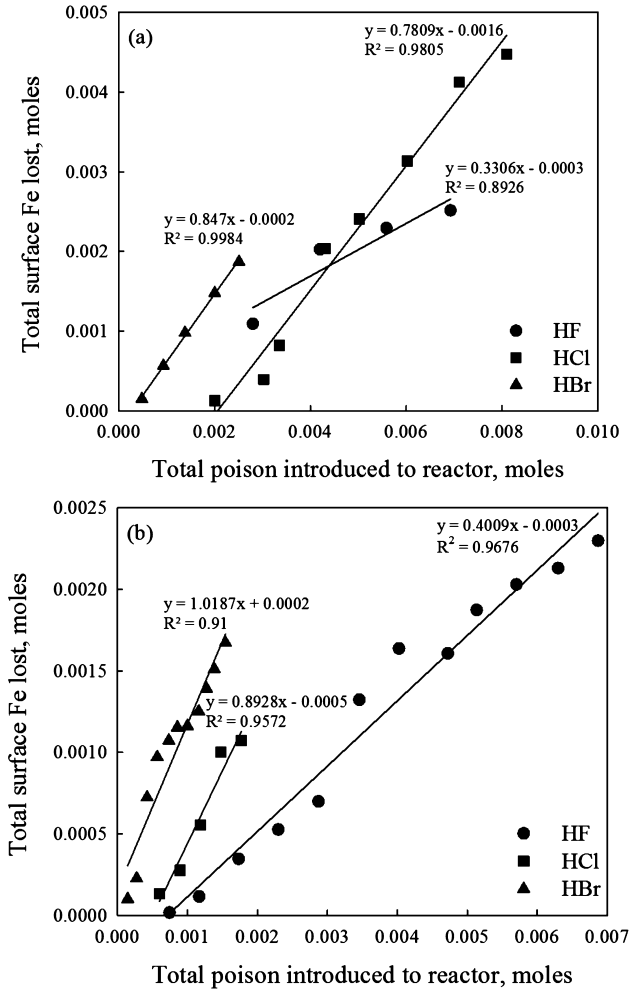

Figure 10. Relationships between the amounts of surface iron lost and the amounts of hydrohalic acid introduced at (a) 270 and (b) 260 °C.

Figure 10 demonstrates two important aspects of the nature of poisoning of Fe by halide ions. Regardless of temperature and type of hydrohalic acid used, the surface Fe and halide ions exhibit good linear relationships in all cases, as indicated by the reasonably high correlation coefficients (R^2 > 0.96 for four data sets and > 0.9 for two data sets). The results suggest that the proposed adsorption and site blocking mechanism most likely accounts for the observed deactivation. In Figure 10a, the Fe/F^-, Fe/Cl^-, and Fe/Br^- ratios are represented by the slopes of different lines and determined to be 0.33, 0.78, and 0.85, which indicate that each F^-, Cl^-, or Br^- ion eliminated 0.33, 0.78, and 0.85 surface Fe atoms, respectively. The differences in the Fe/X^- ratios suggest that the Fe catalysts exhibit different sensitivities to F^-, Cl^-, and Br^- halides; that is, the poisoning strengths of each halide differed. Among the hydrohalic acids tested, HF had the lowest poisoning effect, and HBr had the greatest. The Fe/F^- ratio is less than half that of the other two poisons. Interestingly, the Fe/X ratio determined at 260 °C (Figure 10b) follows precisely the same trend, Fe/F^- < Fe/Cl^- < Fe/Br^-, as that achieved at 270 °C, confirming HF as having the lowest effect among the poisons tested, and HBr having the greatest effect. However, all Fe/F^-, Fe/Cl^-, and Fe/Br^- ratios at 260 °C slightly increased to 0.4, 0.89, and 1.02, which further supports the view that the deactivation proceeded through an adsorption mechanism because the lower the temperature, the more strongly the molecules are adsorbed (i.e., more energy is required to break the chemisorption bond).

3.8. WGS and FTS Rates during Deactivation by HX. As discussed above, adsorption of halide ions (F^-, Cl^-, and Br^-) on the Fe catalyst surface was proposed to be the primary cause of Fe catalyst deactivation by HX. However, the extent to which HX affected WGS and FTS rates is another interesting issue that deserves further discussion because it pertains to the efficiency of carbon usage. Table 5 summarizes the FTS rate and WGS rate before and after adding the hydrohalic acid poisons at the highest concentration levels used (20−40 ppm) in different poisoning runs; moreover, the percentage losses in FTS and WGS rates during deactivation are also provided. In all cases (i.e., HF, HCl, and HBr cofeeding runs), the loss rates for WGS at different temperatures and times on-stream were ∼40−70% higher than that of FTS. This phenomena was observed over a wide range of CO conversion levels. Figure 11a−c shows the changes in the ratio of r_{WGS} to r_{FTS} (r_{WGS}/r_{FTS}), a parameter to measure relative changes in WGS and FTS rates, with the Fe catalyst deactivation rate in the CO conversion range of 70−20% for all three hydrohalic acids tested. The results of all test runs consistently show a greater sensitivity to poisoning for WGS relative to FTS over the entire CO conversion range tested.

Table 5. Summary of WGS Rate, FTS Rate, and Their Percentage Losses Using the Fe Catalyst during Co-Feeding of 20-40 ppm Hydrohalic Acids

poison, level	T, °C	t, h	r_{WGS}, mol/g_{cat}/h	r_{FTS}, mol/g_{cat}/h	WGS rate loss, %	FTS rate loss, %	ratio of WGS rate loss %/FTS rate loss %
30 ppm of HF	270	553	0.0812	0.0973	57.6	34.2	1.68
		673	0.0344	0.0640			
40 ppm of HCl	270	240	0.0901	0.0948	88.4	57	1.55
		432	0.0104	0.0407			
40 ppm of HBr	270	432	0.0575	0.0727	55.1	29.6	1.86
		562	0.0258	0.0512			
20 ppm of HF	260	411	0.0746	0.0868	73.2	44.6	1.64
		719	0.0200	0.0481			
23 ppm of HCl	260	954	0.0252	0.0362	81.0	51.7	1.57
		1100	0.0048	0.0175			
20 ppm of HBr	260	920	0.0515	0.0666	73.7	51.8	1.42
		1178	0.0135	0.0321			

DOI: 10.1021/acscatal.5b00023
ACS Catal. 2015, 5, 3124−3136

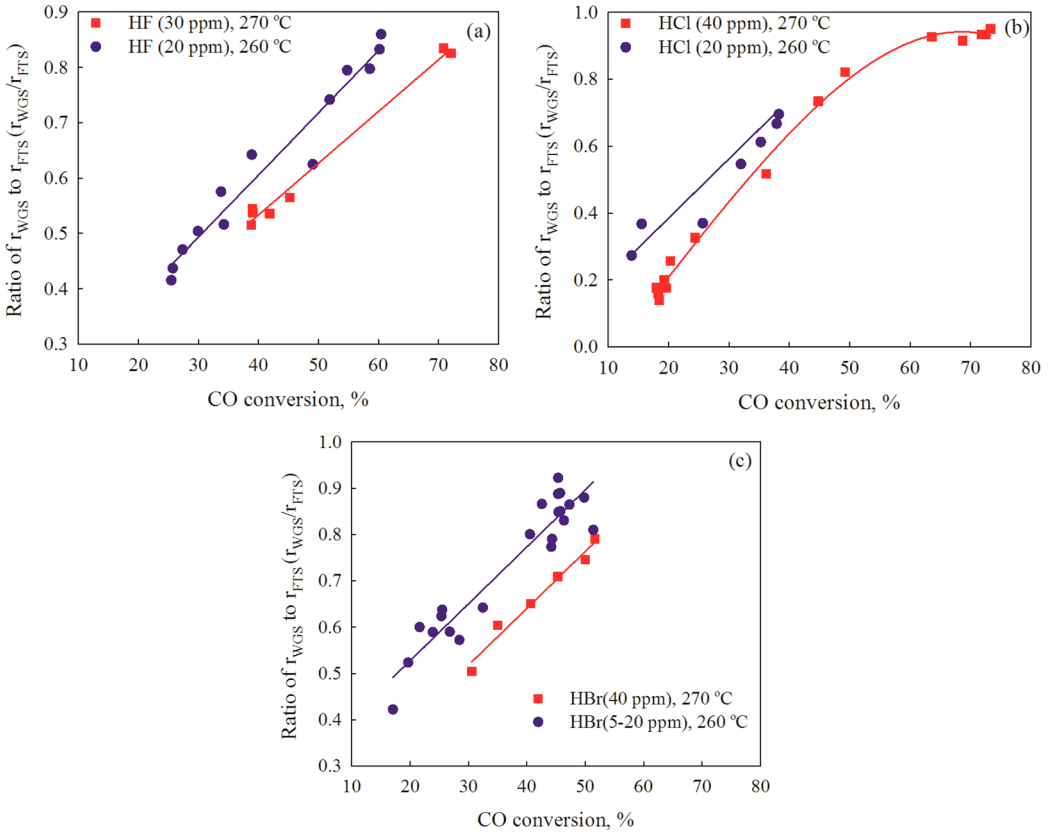

Figure 11. Change in ratio of WGS rate to FTS rate with CO conversion and temperature during adding (a) 20−30 ppm of HF, (b) 20−40 ppm of HCl, (c) 5−40 ppm of HBr on 100 Fe/5.1 Si/2 Cu/3 K. FTS: 1.3 MPa and H_2/CO = 0.67−0.77.

The greater sensitivity to HX exhibited by WGS could be due to a site blocking effect on the pressure factor term in the rate, $r_i = k_i f(p)$.[20] However, this factor can be readily excluded. As shown in Figure 5, decreasing CO conversion of the Fe catalyst from 70 to 20% was accompanied by a rapid increase in the partial pressure of CO (P_{CO}), a moderate increase in the partial pressure of water (P_{H_2O}), and a sharp drop in the partial pressure of CO_2 (P_{CO_2}), and the partial pressure of H_2 (P_{H_2}) was maintained relatively constant. Therefore, the pressure effect from the P_{CO} and P_{H_2O} on the WGS and FTS rates were both nonnegative during the deactivation. This leads to the conclusion that it was HX decreasing the WGS rate constant (k) more than the FTS rate constant that caused a more rapid loss in the WGS rate over the entire range of CO conversions. This deduction is reasonable if the HX poisons cover magnetite and iron carbides at the same probability because magnetite and carbide were generally assumed to be active sites for the FTS and WGS reactions, respectively,[16,21] and magnetite was found to give a higher relative WGS rate constant to the FTS rate on iron carbide.[20] However, our unpublished data indicate that at these low FTS conditions, Fe_3O_4 is a poor WGS catalyst. In addition, the fact that the FTS remains constant while about half of the initial iron carbide is converted to Fe_3O_4 has been interpreted to mean that oxidation occurs at the core of the catalyst particle, leaving a constant surface composition during this conversion. Both of these facts argue against WGS occurring on Fe_3O_4 and FTS on iron carbide.

Because HX poisoning simultaneously decreased the CO_2 rate and CO_2 selectivity in the case of the iron catalyst (Figure 11a−c and Table 5), one may expect that Fe catalyst poisoned by HX may generate lower CO_2 selectivity at the same conversion level. To verify this, CO conversion after testing 30 ppm of HF was brought back to the initial conversion level (70%), where no poison was added, by decreasing space velocity before it was poisoned. It was found that CO_2 selectivity was 46% (before poisoning), but after poisoning, was somewhat lower, 39%, a decrease of 15%. Therefore, there may be an opportunity for using HX poisoning to provide a limited means of controlling carbon usage efficiency because the current data suggest that HX may be used to slightly adjust the WGS activity for the iron catalyst. Additional work is needed to further explore that aspect.

4. CONCLUSIONS

The effect of up to 40 ppm hydrohalic acid (i.e., HX (X = Cl^-, Br^-, and F^-)) in syngas on the performance of a 100 Fe/5.1 Si/2 Cu/3 K FTS catalyst was investigated. The activity and selectivity trends, threshold limits of the contaminants, and HX poisoning mechanism, including the relationship between the surface Fe and HX poison (Fe/X^-), were examined.

The limits of HX acids were identified at 260 and 270 °C by online cofeeding different levels of HX, starting from 0.1 ppm. The results from HX poisoning for 72−170 h indicate that ~2 ppm of HCl or HBr is problematic for the 100 Fe/5.1 Si/3 K/2 Cu catalyst, and increasing the levels of HCl or HBr to the 3−5 ppm range results in a low to moderate extent of deactivation. However, a higher limit, 10 ppm, was found for HF. For all three hydrohalic acids, at a high level of 20+ ppm of HX, the catalyst experiences rapid deactivation.

The CH_4, C_{5+}, and CO_2 selectivities changed significantly when high levels of HX (i.e., 20+ ppm) were cofed. The CH_4

DOI: 10.1021/acscatal.5b00023
ACS Catal. 2015, 5, 3124−3136

selectivity increased, and C_{5+} and CO_2 selectivities decreased with time. However, the total C_4 olefin and 1-C_4 olefin changed very little when the Fe catalyst was exposed to HX. It is postulated that the halide ions adsorbed onto the Fe catalyst surface and hindered CO adsorption to influence product selectivity trends.

The mechanism by which high levels of HX deactivated the Fe catalyst was studied by XRD and Mössbauer spectroscopy. Both XRD and Mössbauer spectroscopy results revealed the presence of iron carbides and magnetite in the Fe catalyst after CO carburization (activation) and during FTS. The Mössbauer spectroscopy results further showed that the total iron carbide content (i.e., χ-Fe_5C_2 + ε'-$Fe_{2.2}C$) did not change significantly before and after cofeeding HX, regardless of temperature, which supports the view that HX sorption and subsequent blocking of Fe sites was the primary cause of catalyst deactivation. The relationship between surface Fe and halide ions introduced (Fe/X^-) was found to be linear for all HX acids at different conditions, consistent with the proposed site-blocking mechanism. Moreover, the Mössbauer spectroscopy results suggest that phase transformations took place during the startup and deactivation periods. A fraction of χ-Fe_5C_2 converted to Fe_3O_4 or ε'-$Fe_{2.2}C$ in the two periods, respectively. This was attributed to changes in conditions, including temperature, as well as the partial pressures of water, CO, and H_2 during the startup and deactivation periods.

HF, HCl, and HBr were found to exert different poisoning impacts on the Fe catalyst, which was revealed by differences in the Fe/X^- (surface Fe poisoned based on activity decrease/X^- added) values obtained. The Fe/F^-, Fe/Cl^-, and Fe/Br^- ratios at 270 °C were 0.33, 0.78 and 0.85, respectively, and they were correspondingly higher (i.e., 0.4, 0.9, and 1.01) at 260 °C. The higher Fe/X^- values at the lower temperature are consistent with the view that sorption and site-blocking were responsible for Fe catalyst deactivation by hydrohalic acids. At both temperatures, the Fe/X^- ratio follows the trend: $Fe/F^- < Fe/Cl^- < Fe/Br^-$, suggesting that F^- gave the lowest poisoning effect, and Br^-, the greatest. This is in line with the higher threshold limit identified for HF. Differences in poisoning ability is a complicated issue and could be related to the size of the ions, electronegativity, ion density, or a combination thereof.

Adding 20−40 ppm of HX in the feed led to faster decreases in WGS activity than that of FTS during the entire deactivation period (and CO conversion range, X_{CO} = 70−20%) studied. This result suggests that HX addition may be used to provide at least a certain degree control of CO_2 selectivity as relates to carbon usage efficiency. This is an important topic for improving FTS processes with typically low H_2/CO feeds (e.g., BTL or CTL processes).

AUTHOR INFORMATION

Corresponding Author

*Phone: 859-257-0251. E-mail: burtron.davis@uky.edu.

Notes

The authors declare no competing financial interest.

ACKNOWLEDGMENTS

This work was made possible by financial support from the U.S. DOE (Contract No. DE-FC26-08NT0006368) and the Commonwealth of Kentucky.

REFERENCES

(1) van Steen, E.; Claeys, M. *Chem. Eng. Technol.* **2008**, *31*, 655−666.
(2) Lillebo, A. H.; Holmen, A.; Enger, B. C.; Blekkan, E. A. *Energy and Environment* **2013**, *2*, 507−524.
(3) Ma, W. P.; Jacobs, G.; Kang, J.; Sparks, D.; Shafer, W.; Davis, B. H. *Fischer−Tropsch synthesis: Effect of ammonia and H_2S in syngas on the Fischer−Tropsch performance of a precipitated iron catalyst*; AICHE Annual Meeting, Minneapolis, MN, October 16−21, 2011.
(4) Sparks, D. E.; Jacobs, G.; Gnanamani, M. K.; Pendyala, V. R. R.; Ma, W.; Kang, J.; Shafer, W. D.; Keogh, R. A.; Graham, U. M.; Gao, P.; Davis, B. H. *Catal. Today* **2013**, *215*, 67−72.
(5) Ma, W.; Jacobs, G.; Kang, J.; Sparks, D. E.; Gnanamani, M. K.; Pendyala, V. R. R.; Shafer, W. D.; Keogh, R. A.; Graham, U. M.; Thomas, G. A.; Davis, B. H. *Catal. Today* **2013**, *215*, 73−79.
(6) Pendyala, V. R. R.; Gnanamani, K.; Jacobs, G.; Ma, W. P.; Shafer, W. D.; Davis, B. H. *Appl. Catal., A* **2013**, *468*, 38−43.
(7) Ma, W.; Jacobs, G.; Sparks, D. E.; Pendyala, V. R. R.; Hopps, S.; Thomas, G. A.; Davis, B. H.; Hamdeh, H. H.; MacLennan, A.; Hu, Y. *J. Catal.*, DOI: 10.1016/j.jcat.2015.04.004.
(8) Huynh, C.V.; Kong, S.-C. *Fuel* **2013**, *107*, 455−464.
(9) Robota, H. J.; Alger, J.; Pretorius P. J. *Impact of low levels of ammonia in syngas on the Fischer−Tropsch synthesis performance of cobalt and iron catalysts in fixed-bed operation*; National Spring Meeting of the American Institute of Chemical Engineers, Houston, TX, April 1−5, 2012.
(10) Davis, B. H. *Technology development for iron Fischer−Tropsch catalysis*; Department of Energy final report; Department of Energy: Washington, DC, 1998.
(11) Davis, B. H.; Jacobs, G. *Sensitivity of Fischer−Tropsch synthesis and water-gas shift catalysts to poisons from high-temperature high-pressure entrained-flow (EF) oxygen blown gasifier gasification of coal/biomass mixtures*; Department of Energy final report; Department of Energy: Washington, DC, 2011.
(12) Raje, A. P.; O'Brien, R. J.; Davis, B. H. *J. Catal.* **1998**, *180*, 36−43.
(13) Yang, J.; Ma, W. P.; Chen, D.; Holmen, D.; Davis, B. H. *Appl. Catal., A* **2014**, *470*, 250−260.
(14) Herzog, K.; Gaube, J. *J. Catal.* **1989**, *115*, 337−346.
(15) Gaube, J.; Klein, H. F. *Appl. Catal., A* **2008**, *350*, 126−132.
(16) Amelse, J. A.; Schwartz, L. H.; Butt, J. B. *J. Catal.* **1981**, *72*, 95−110.
(17) Borg, O.; Hammer, N.; Enger, B. C.; Myrstad, R.; Lindv, O. A.; Eri, S.; Skagseth, T. H.; Rytter, E. *J. Catal.* **2011**, *279*, 163−173.
(18) Hofer, L. J. E. Crystal phases and their relation to Fischer−Tropsch catalysts. In *Catalysis*; Emmett, P. H., Ed.; Van Nostrand-Reinhold: New York, 1956; Vol. *IV*; pp427.
(19) Jung, H. J.; Vannice, M. A.; Mulay, L. N.; Stanfield, R. M.; Delgass, W. N. *J. Catal.* **1982**, *76*, 208−224.
(20) Ma, W.; Jacobs, G.; Graham, U. M.; Davis, B. H. *Top. Catal.* **2014**, *57*, 561−571.
(21) Malessa, R.; Baerns, M. *Ind. Eng. Chem. Res.* **1988**, *27*, 279−283.

DOI: 10.1021/acscatal.5b00023
ACS Catal. 2015, 5, 3124−3136